JOURNAL OF MATERIALS SCIENCE 5 (1970) 141-148

Precipitation of Magnesium Ferrite from MgO-Fe$_x$O Solid Solutions*

S. K. EVANS†, I. B. CUTLER
Division of Materials Science and Engineering, University of Utah, Salt Lake City, Utah, USA

Debye-Scherrer X-ray powder photographs and photomicrographs of samples in the MgO-Fe$_x$O system have revealed the possible presence of spinodal decomposition.

Samples of MgO doped with 4.99 cation % iron were quenched from high temperature into water. Debye-Scherrer photographs taken after quenching revealed the presence of satellite lines located adjacent to the main diffraction lines. These lines can be interpreted as due to a periodic fluctuation in lattice parameter. This periodic fluctuation has been described as one of the distinguishing features of spinodal decomposition.

Microstructures of the samples in correlation with electrical conductivity measurements revealed two different types of precipitation depending on sample heat-treatment. The first type reveals $MgFe_2O_4$ precipitates at grain-boundaries. The second reveals a grainy precipitate network permeating the structure. The grainy network could be due possibly to growth of precipitates following an initial decomposition of the spinodal type.

1. Introduction

Phase transformations in solids usually occur by means of nucleation and growth of crystalline phases at lattice imperfections and surfaces. In certain cases, however, decomposition can take place by amplification of certain coherent composition fluctuations within the bulk of the material. This decomposition is thermodynamically possible within the region of a binary phase diagram defined by

$$\left(\frac{\partial^2 f}{\partial c^2}\right)_{T,P} < 0,$$

where f is the Gibbs free energy per mole of solution and c is the composition. This region is represented graphically in fig. 1. The spinodal is indicated and is defined by the locus of points where

$$\left(\frac{\partial^2 f}{\partial c^2}\right)_{T,P} < 0.$$

The region of coherent decomposition is called spinodal decomposition because it lies within the region bounded by the spinodals.

In recent years a number of workers have described the basic features of spinodal decomposition and have proposed ways of determining its existence experimentally. Fine [1] discusses the basic theory and its relationships to homogeneous and heterogeneous nucleation. Hillert [2] treated spinodal decomposition as a periodic composition fluctuation in one dimension in an inhomogeneous solid solution. Cahn [3, 4] has extended Hillert's treatment to three dimensions and has treated cubic crystals as well. Recently

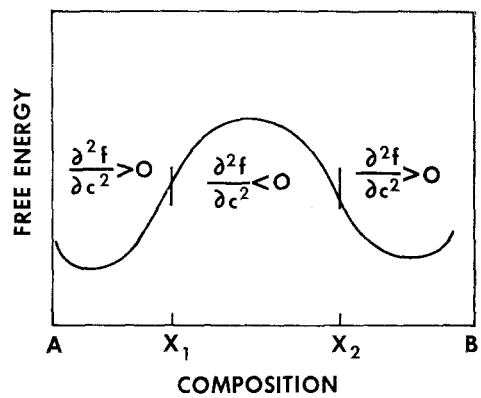

Figure 1 Gibbs free energy per mole vs. composition for a binary system with a miscibility gap.

*Based on a thesis submitted by S. K. Evans for the Ph.D. degree in ceramic engineering, University of Utah, September 1965.
†Now a ceramist at General Electric Company, Vallecitos Nuclear Center, Pleasanton, California 94566, USA.

Cahn [5] and Huston, Cahn and Hilliard [6] have extended the treatment to include decomposition during continuous cooling and the later stages of decomposition leading to the beginnings of particle coarsening.

1.1. Elements of the Theory

Spinodal decomposition begins as an infinitesimal composition fluctuation spread over the extent of the crystal. As the decomposition proceeds, an amplification of certain wavelength components of the fluctuation results. In cubic crystals, the amplification takes on the three {1 0 0} planes or the four {1 1 1} planes, depending upon the elastic constants of the material. This gives rise in the {1 0 0} case to an interlocking network of <1 0 0> rods, alternately enriched and depleted in one of the components. The {1 1 1} case produces cubes of alternately enriched and depleted material along the <1 0 0> directions.

Since the most convenient experimental analysis of spinodal decomposition includes continuous cooling of the experimental materials, it is instructive to examine the resulting structures in relation to the quenching rates involved. At high cooling rates, the degree of decomposition may be too small to be detected. In opposition to this, at slow cooling rates, the decomposition may be completed during the quench. There is an intermediate region where partial decomposition occurs during cooling. In this region, the wavelength with the maximum amplification is not affected by changes in quenching rate. In the region of slower quenching, however, the magnitude of the wavelength is inversely proportional to the one-sixth power of the quench rate.

1.2. System Properties

Several workers have studied the phase relationships in the magnesium oxide-iron oxide system. Phillips, Somiya and Muan [7] have investigated the system at high temperatures in air. The results of their work are shown in fig. 2. The portions of the phase diagram below 50 wt % are only estimates.

Groves and Fine [8] have conducted a study of solid solution and precipitation hardening in Mg-Fe-O alloys. They found that doping single crystal MgO with small amounts of iron increased its flow stress by a factor of three upon quenching in air after heat-treatment at 1400° C in air. The hardening was attributed to Fe^{3+} in solid solution, since they found that maximum

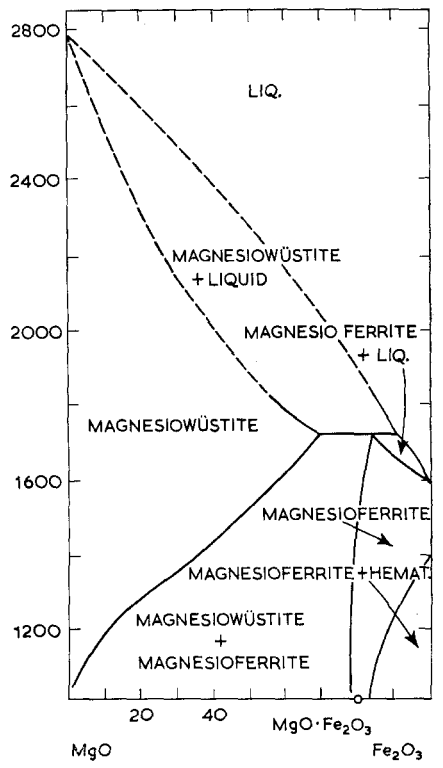

Figure 2 System $MgO\text{-}Fe_2O_3$ in air [7].

hardening occurred after only 7.5 min of ageing in air at 800° C, and additional annealing at temperatures where precipitates were expected to form served to coarsen the precipitate and decrease the strength. They observed octahedral precipitate particles in all air-annealed crystals with the faces of the octahedra being parallel to the {1 1 1} planes in the MgO.

The magnetic properties of the $MgO\text{-}MgFe_2O_4$ system have been investigated by Wirtz and Fine [9, 10] and Woods and Fine [11]. Wirtz and Fine [10] concluded that superparamagnetism in MgO containing 1.0 cation % of Fe is the result of precipitation of $MgFe_2O_4$ particles during ageing at 700 to 800° C in air following an air-quench from 1440° C. They indicated that the Fe^{3+} ions remained in solid solution during the quench. Woods and Fine extended the previous magnetic treatment, concluding that small superparamagnetic islands existed in 0.9 cation % of Fe in MgO following a water-quench from a 1400° C air heat-treatment. They were unable to detect these small precipitates by transmission electron microscopy, X-ray diffraction or electron diffraction.

McCollister and Van Vlack [12] have studied microstructures for various heat-treatments in the MgO-$MgFe_2O_4$ system. They report three different distributions of precipitate particles depending upon the thermal history of the samples tested. They report precipitates existing as (i) grain-boundary networks; (ii) Widmanstatten patterns within the grains; or (iii) spheroidised precipitates. The latter appeared to be induced by extension of the annealing times for producing the Widmanstatten structure. The microstructures strongly suggest that $MgFe_2O_4$ precipitates along the {1 0 0} planes.

1.3. X-Ray Diffraction Sidebands

The theory of spinodal decomposition postulates that coherent precipitates appear as a sinusoidally varying concentration gradient throughout the extent of the crystal lattice. In order to determine experimentally whether spinodal decomposition has taken place in a system, it is necessary to detect the change in lattice characteristics resulting from the decomposition. Several workers have investigated the problem of X-ray diffraction from a sinusoidally distorted lattice. Dehlinger [13] and Kochendorfer [14] treated the problem rigorously, finding that the main diffraction lines would be replaced by groups of lines where satellites or sidebands surrounded the main lines. Daniel and Lipson [15], in seeking to reduce the theory to experimentally determinable parameters, predicted that the main diffraction lines would be flanked by two side-bands of equal intensity. They derived the following expression for the wavelength of a periodic structure in terms of the positions of the side-bands on a Debye-Scherrer photograph

$$Q = \frac{h \tan \theta}{(h^2 + k^2 + l^2)\,\Delta\theta}$$

where h, k and l are the Miller indices; θ is the diffraction angle, $\Delta\theta$ is the angular distance between the main diffraction line and the first sideband, and Q is the wavelength of the periodic structure. Hargreaves [16] and Tiedema, Bouman and Burgers [17] have treated variations of the theory to include asymmetrical alloys.

Peculiarities in measurement of electrical conductivity versus temperature on samples of magnesium oxide containing iron led the authors to consider modes of precipitation which take place extremely rapidly and result in the production of widely varied precipitate microstructures whose characteristics are strongly dependent upon prior heat-treatment. X-ray diffraction studies were initiated which provided evidence of sidebands for certain heat-treatments resulting in the claim that spinodal decomposition takes place in the magnesium oxide-iron oxide system.

2. Experimental Technique

Samples of magnesium oxide containing 4.99 cation % iron were prepared by mixing Baker and Adamson reagent grade Fe_2O_3 and Mallinckrodt reagent grade MgO powders in appropriate amounts. Water was added to hydrate the mixtures and to aid in mixing. The mixtures were then calcined at 1100° C in air to produce a sinterable material. The powders thus obtained were pressed into discs and fired at 1640° C for 1 h. The discs were 92% dense with a grain size of approximately 25 μm. After sintering, the discs were cut into rectangular prisms with a diamond saw. Samples for metallographic analysis were mounted in bakelite following appropriate heat-treatments. Samples for X-ray powder analysis were pulverised and screened through a 325 mesh sieve.

Debye-Scherrer photographs were made using a 5.73 cm radius Debye-Scherrer camera and Cu radiation. Heat-treatments were performed in a vertical tube furnace using silicon carbide heating elements. The furnace atmosphere at all times was air.

Following sintering, the samples were given heat-treatments based upon their intended uses. Samples for quenching were heated to 1410° C in air, a high enough temperature to dissolve any spinel precipitates, then dropped into water at 20° C within 1 sec after leaving the furnace hot zone.

Electrical measurements were carried out in the same furnace. A four-terminal method was used for measuring electrical conductivity. Voltage measurements were made with two Keithley electrometers, models 610 and 621, to maximise input impedance.

3. Results

3.1. Debye-Scherrer Photographs

Debye-Scherrer photographs were prepared from specimens of MgO containing 4.99 cation % iron. Fig. 3 shows the Debye-Scherrer photograph of a specimen annealed for 1 h at 1350° C and then quenched into water. The Debye-Scherrer photograph of pure MgO is shown for comparison in fig. 4. Several sidebands are

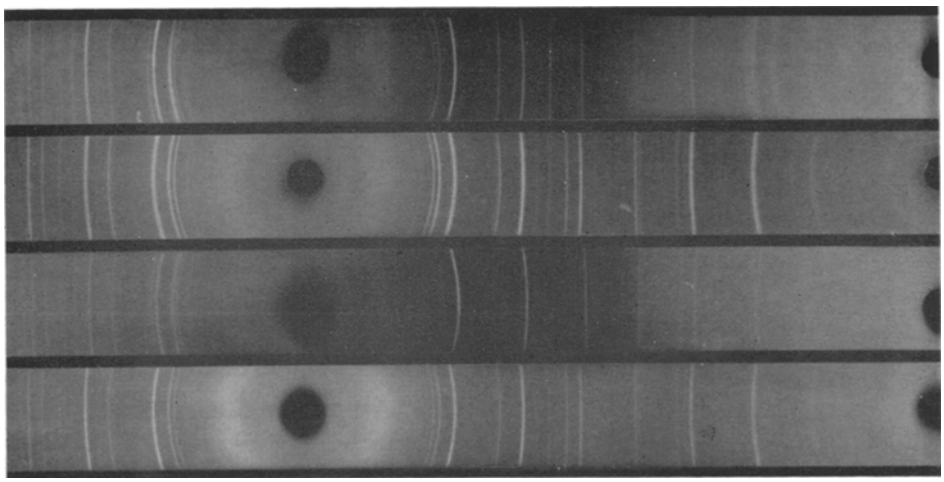

Figure 3 Debye-Scherrer photograph of MgO specimen containing 4.99 cation % iron annealed for 1 h at 1350° C and then quenched into water.
Figure 4 Debye-Scherrer photograph of pure MgO.
Figure 5 Debye-Scherrer photograph of MgO specimen containing 4.99 cation % iron annealed for 1 h at 1350° C, quenched into water, then reheated for 5 min at 475° C.
Figure 6 Debye-Scherrer photograph of MgO specimen containing 4.99 cation % iron annealed for 1 h at 1350° C, quenched into water, then reheated for 2 h at 475° C.

observable in fig. 3. These sidebands have been identified as belonging to the 111 Kα, 111 Kβ, 200 Kα, 511 Kβ, and 422 Kα diffraction lines. Their corresponding periodic structure wavelengths, as determined by Daniel and Lipson's formula, are given in table I. Fig. 5 shows the Debye-Scherrer photograph of a specimen annealed for 1 h at 1350° C, quenched in water, then reheated for 5 min at 475° C. Sidebands to the same lines as before are visible in this specimen. The corresponding wavelengths are given in table II. Fig. 6 shows the Debye-Scherrer photograph of a specimen annealed for 1 h at 1350° C, then quenched in water, followed by a two-hour anneal at 475° C. No sidebands are evident, indicating that their cause has been somehow eliminated.

TABLE I Wavelength of periodic structure for an MgO specimen containing 4.99 cation % iron quenched from 1350° C

Diffraction lines	Q	Wavelength, Å
111 Kβ	12.9	54.3
111 Kα	11.1	46.7
200 Kα	13.6	57.2
511 Kβ	5.1	21.3
422 Kα	6.5	27.3

TABLE II Wavelength of periodic structure for an MgO specimen containing 4.99 cation % iron quenched from 1350° C then reheated for 5 min at 475° C

Diffraction lines	Q	Wavelength, Å
111 Kβ	12.8	53.8
111 Kα	11.7	48.2
200 Kα	12.2	51.3
511 Kβ	5.3	22.3
422 Kα	6.8	28.6

3.2. Electrical Conductivity Measurements

Electrical conductivity measurements were made on samples of MgO containing 4.99 cation % iron following annealing at 1400° C for 2 h. Measurements were made at intervals while decreasing the temperature from 1400° C slowly. The results of these measurements are shown in fig. 7. At 1150° C, the conductivity dropped abruptly by a factor of four. The decrease was observed to take place in a time period of the order of 1 sec. At about 1000° C the conductivity rose slightly and formed a lower temperature leg with a much lower activation energy for conduction than the high temperature region. The room temperature colour of the sample following this measurement was chocolate brown.

The same sample was quenched rapidly into water from air-heating at 1400° C. Following the quench, the sample colour was green. Electrical

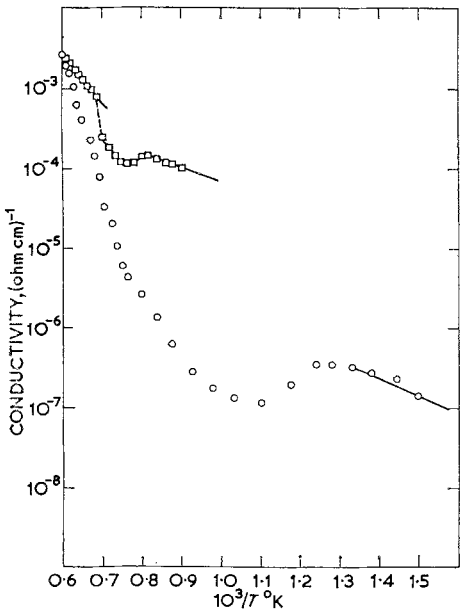

Figure 7 Electrical conductivity vs. $1/T$ for MgO specimen containing 4.99 cation % iron. (Circles represent increasing temperature measurements; squares represent decreasing temperature measurements.)

conductivity measurements made with increasing temperature from room temperature with this sample revealed a peak in the conductivity at 500° C. At or near this peak, the sample colour began to change to brown. With further increasing temperatures a rather irregular curve was evident up to nearly 1400° C where the increasing and decreasing temperature curves became co-linear.

The colour change is a very characteristic feature of the precipitation process. Solid solutions in their quenched condition vary from light to dark green in colour, depending on the iron oxide content. Annealed at approximately 500 to 600° C, these same samples quickly (< 5 min) turn light to dark brown, depending on their iron oxide content. The colour change is uniform throughout the cross-sections of these dense samples and far below the temperature at which oxidation of solid solutions has been reported by Schaefer and Brindley [18] and Ficalora and Brindley [19]. Oxidation was observed by Brindley and co-workers at the surface as a slow, diffusion-controlled process that was measured at temperatures in the neighbourhood of 1000° C.

3.3. Microstructures

Ceramographic specimens were prepared representing several pertinent regions in the electrical

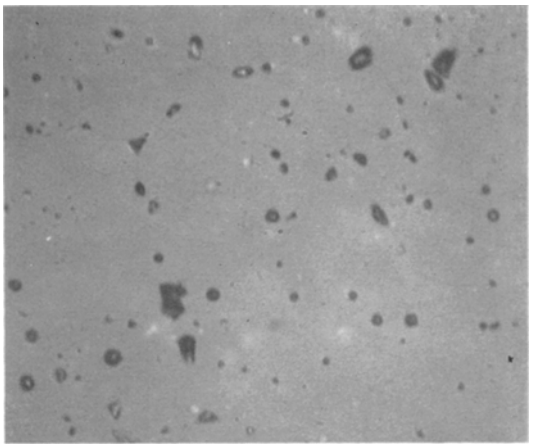

Figure 8 Microstructure of MgO specimen containing 4.99 cation % iron quenched into water after annealing at 1400° C for 1 h.

conductivity versus temperature curves. Fig. 8 shows the polished surface of a specimen of MgO containing 4.99 cation % iron quenched into water after annealing at 1400° C for 1 h in air. No second phase is observable in the microstructure. The corresponding region of the conductivity curve is higher in temperature than the initial rapid decrease in conductivity.

Fig. 9 shows the microstructure of a specimen of MgO containing 4.99 cation % iron quenched into water from 1410° C, then reheated at 1159° C in air for 1.5 h. A magnesium ferrite second phase is observable at grain-boundaries. The corresponding region in the conductivity curve is just below the conductivity drop temperature, but

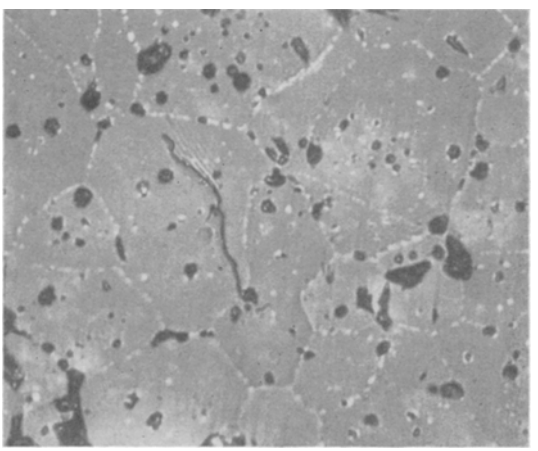

Figure 9 Microstructure of MgO specimen containing 4.99 cation % iron quenched into water from 1410° C, then reheated at 1159° C in air for 1.5 h.

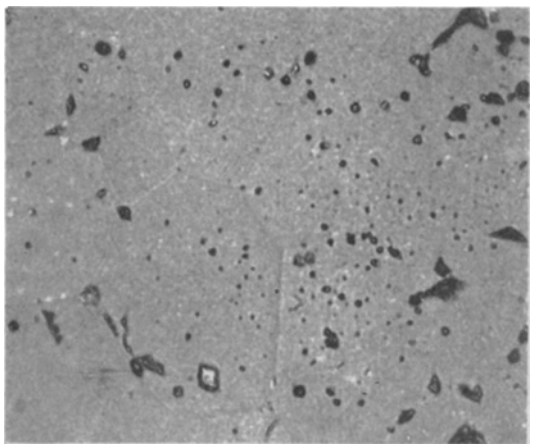

Figure 10 Microstructure of MgO specimen containing 4.99 cation % iron quenched into water from 1410° C, then annealed for 2.25 h at 964° C.

above the knee in the curve at 1000° C. The X-ray diffractometer pattern reveals the presence of $MgFe_2O_4$ peaks.

Fig. 10 shows the result of quenching a specimen of MgO containing 4.99 cation % iron in water after annealing for 1 h at 1410° C, then annealing for 2.25 h at 964° C. Precipitates of magnesium ferrite again are visible but form a grain structure which permeates the bulk of the MgO without regard for grain-boundaries. The corresponding region of the conductivity curve is above the peak temperature of 500° C in the increasing temperature plot.

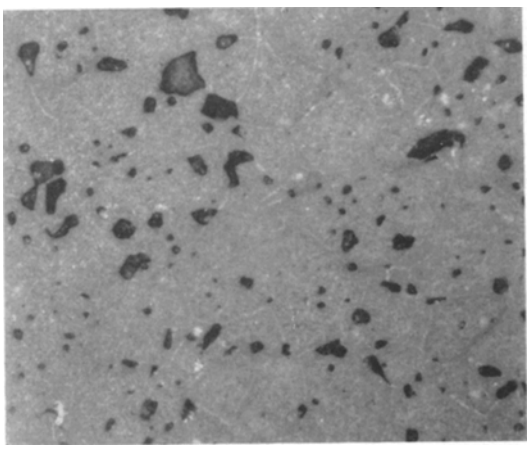

Figure 11 Microstructure of MgO specimen containing 4.99 cation % iron quenched into water from 1410° C, then annealed for 1 h at 1018° C.

The microstructure in fig. 11 illustrates the result of quenching a specimen of MgO containing 4.99 cation % iron in water following an anneal at 1410° C for 1 h, then reheating at 1018° C for 1 h. The grainy precipitate structure evident in the preceding photograph is also present here, along with some precipitates occupying grain-boundary positions. The conductivity region represented here is slightly higher in temperature than the preceding one.

3.4. Magnetic Moment Measurements

Magnetic moment measurements, using the method of Rathenau and Snoek [20], were performed on specimens of MgO containing 4.99 cation % iron. The magnetic moment increased from 10^{-3} Bohr magnetons per molecule in a specimen quenched from 1350° C into water to 6×10^{-2} Bohr magnetons per molecule in the same specimen after annealing for 2 h at 900° C. The large increase in magnetic moment indicates a clustering of ferrimagnetic material during annealing at 900° C, similar to that reported by Wirtz and Fine [10]. This material is most likely magnesium ferrite.

4. Discussion

The presence of sidebands in the Debye-Scherrer photographs implies that a spinodal decomposition has taken place in MgO containing 4.99 cation % Fe during water quenching following a 1400° C heat-treatment in air. The following discussion describes what may have taken place as a result of programmed heat-treatments.

The X-ray photograph in fig. 3 indicates that a periodic structure has been formed during the quench with a wavelength of about 50 Å. It is suggested that this periodic structure is due to spinodal decomposition as described by Cahn and others. The optical microscope cannot resolve such a structure, so the microstructure appears to represent a solid solution of iron in MgO as represented in fig. 8. Since the spinel structure shares the same oxygen sublattice with MgO, $MgFe_2O_4$ can be constructed from MgO with iron in solution by clustering Fe^{3+} ions with Mg^{2+} vacancies, then moving approximately half of the Fe^{3+} ions to tetrahedral interstices. Apparently this precipitation forms by amplification of infinitesimal composition fluctuations throughout the lattice, resulting in a periodic structure. The structure persists at low temperatures until heating above about 500° C takes

place. At this temperature, the initial coherent precipitates begin to coarsen and form discrete interfaces with the rest of the lattice. The low temperature electrical conductivity is thus indicative of the initial spinodal decomposition involving localised shifting of Fe^{3+} ions to tetrahedral lattice sites but still no gross diffusion of iron to discrete precipitate complexes. As the temperature reaches approximately 500° C, thermal activation is sufficient to begin substantial migration of iron to the iron-rich regions of the periodic structure. This results in a network of small $MgFe_2O_4$ precipitates in an iron-depleted MgO matrix. The discreteness comes about through narrowing the width of the Fe^{3+} concentration gradient from the initial sinusoidal condition to a discrete precipitate boundary as the periodic structure deteriorates and the precipitate coarsens. The depletion of the Fe^{3+} from the matrix results in a decrease in the electrical conductivity of the continuous matrix phase. The formation of the discrete precipitate causes disappearance of sidebands in the Debye-Scherrer photographs as illustrated in fig. 6. Also, the magnetic moment measurements indicate a clustering of ferrimagnetic material for specimens undergoing the green to brown colour change which occurs at this same temperature.

The electrical conductivity begins to increase with apparent changing activation energy as the temperature is raised further, indicating an increase in the iron solubility limit in MgO as the temperature is raised. Fig. 10 shows the microstructure indicative of this region at 964° C. The grainy precipitate appearance is probably due to the result of extensive coarsening of the initial spinodal precipitates. The microstructure at a slightly higher temperature (fig. 11) shows the beginning of precipitate migration to grain-boundaries.

A comparison of the microstructure in fig. 9 with electrical conductivity measurements for the highest temperatures in the vicinity of the abrupt drop in conductivity indicates that the conductivity drop is associated with a precipitation of $MgFe_2O_4$ along grain-boundaries. The precipitates form a discontinuous network, depleting iron from the immediate areas in the grains, forming a high resistivity shell around individual grains. The change in activation energy for conduction upon decreasing the temperature further is probably due to a sufficient coarsening of the precipitate so that a continuous network is formed, resulting in a high conductivity path in the $MgFe_2O_4$. The activation energy observed agrees well with Schröder's [21] data on conductivity in magnesium ferrite.

The mechanism of spinodal decomposition is at all times competitive kinetically with the nucleation and growth of precipitates at structural defects. Consider the theoretical binary phase diagram for two solids with a solubility gap. The spinodal or coherent phase boundary lies inside the incoherent boundary ordinarily shown. Outside the spinodal boundary, spinodal decomposition is not possible; there the nucleation and growth precipitation mechanism is paramount. Inside the coherent phase boundary, however, while spinodal decomposition can take place, heterogeneous nucleation can also take place at lattice defects where the free energy is favourable. In MgO containing 4.99 cation % iron, apparently the spinodal decomposition mechanism is more rapid than nucleation and growth, during rapid quenching from high temperatures. During slower cooling, however, nucleation takes place at grain-boundaries before the spinodal phase boundary is crossed as shown in fig. 9. Once the periodic structure is formed during quenching, larger precipitates can form by growth of the initial coherent precipitates accompanied by appearance of incoherent interfaces at fairly low temperatures, or by diffusion of iron to lattice defects at higher temperatures.

It is doubtful whether water-quenching is rapid enough to prevent precipitation at very high iron contents as evidenced from the work of McCollister and Van Vlack. The present study is consistent with the observation made by McCollister and Van Vlack that at the higher temperatures, grain-boundary nucleation becomes competitive with spinodal decomposition in the grain interior.

From the evidence gained in this study, it is impossible to prove that spinodal decomposition has taken place in the quenched solid solutions. However, no other explanation is known that can explain the very rapid formation of a coherent precipitate at low temperatures. Either spinodal decomposition is the mechanism responsible for formation of extremely small precipitates of $MgFe_2O_4$ uniformly throughout the polycrystalline solid solutions (without regard to grain-boundaries, etc.), or another mechanism of nucleation, at present unknown, but of characteristics similar to spinodal decomposition, is responsible for the very rapid nucleation described here.

5. Summary

Debye-Scherrer powder photographs have revealed sidebands to the major diffraction lines which indicate the presence of a periodic structure in samples of MgO containing 4.99 cation % iron following quenching from high temperatures.

Photomicrographs of specimens in correlation with electrical conductivity measurements indicate that two types of precipitation occur in iron-doped MgO when subjected to different heat-treatments.

Quenching from high temperatures produces a microstructure which appears to be a single phase solid solution. Upon reheating at intermediate temperatures, a very fine-grained precipitate appears which is suggestive of coarsening of an initial coherent composition fluctuation. If the reheating is carried out at still higher temperatures, precipitation of magnesium ferrite spinel occurs at grain-boundaries and gross crystal defects. The electrical measurements predict this precipitation by exhibiting a sharp decrease in conductivity when the iron is precipitated at the grain-boundaries. The precipitate coarsening at lower temperatures is also confirmed by the decrease in conductivity at these temperatures following quenching. The colour change from green to brown supports the evidence in this temperature region.

The sixty-fold increase in magnetic moment resulting from the low-temperature electrical and optical transition indicates that a clustering of ferrimagnetic crystallites takes place during the transition.

The reported experimental data indicate that a spinodal decomposition may be taking place in magnesium oxide containing 4.99 cation % iron during quenching of this material from a single phase region. The data suggest that subsequent electrical, optical and magnetic properties in this material are affected greatly by this decomposition.

Acknowledgement

This work was sponsored by the United States Atomic Energy Commission under Contract AT(11-1)-1122.

References

1. M. E. FINE, "Phase Transformations in Condensed Systems" (Macmillan, London, 1964) pp. 70-75.
2. M. HILLERT, *Acta Met.* **9** (1961) 525.
3. J. W. CAHN, *ibid* 795.
4. *Idem, ibid* **10** (1962) 179.
5. *Idem, ibid* **14** (1966) 1685.
6. E. L. HUSTON, J. W. CAHN, and J. E. HILLIARD, *ibid* 1053.
7. B. PHILLIPS, S. SOMIYA, and A. MUAN, *J. Amer. Ceram. Soc.* **44** 167.
8. G. W. GROVES and M. E. FINE, *J. Appl. Phys.* **35** (1964) 3587.
9. G. P. WIRTZ and M. E. FINE, *ibid* **38** (1967) 3729.
10. *Idem, J. Amer. Ceram. Soc.* **51** (1968) 402.
11. K. N. WOODS and M. E. FINE, *ibid* **52** (1969) 186.
12. C. K. MCCOLLISTER and L. H. VAN VLACK, *Bull. Am. Ceram. Soc.* **44** (1965) 915.
13. U. DEHLINGER, *Z. Krist.* **65** (1927) 615.
14. A. KOCHENDORFER, *ibid* **101** (1939) 149.
15. V. DANIEL and H. LIPSON, *Proc. Roy. Soc.* **A181** (1943) 368.
16. M. E. HARGREAVES, *Acta Cryst.* **4** (1951) 301.
17. T. J. TIEDEMA, J. BOUMAN, and W. G. BURGERS, *Acta Met.* **5** (1957) 310.
18. W. L. SCHAEFER and W. G. BRINDLEY, *J. Phys. Chem. Solids* **24** (1963) 919.
19. P. J. FICALORA and G. W. BRINDLEY, *J. Amer. Ceram. Soc.* **50** (1967) 662.
20. G. W. RATHENAU and J. L. SNOEK, *Phillips Res. Repts.* **1** (1946) 239.
21. H. SCHRÖDER, *Z. Chem.* **2** (1962) 94.

Received 17 March and accepted 2 October 1969.